

Available online at www.sciencedirect.com**ScienceDirect**

Procedia CIRP 55 (2016) 101 – 108

www.elsevier.com/locate/procedia

5th CIRP Global Web Conference Research and Innovation for Future Production

Development of a deposition strategy in Cold Spray for Additive Manufacturing to minimize residual stresses

G. Benenati and R. Lupoi*

*Trinity College of Dublin, The University of Dublin, Department of Mechanical and Manufacturing Engineering, Parsons Building, Dublin 2, Ireland** Corresponding author. Tel.: +353 1896 1729; E-mail address: lupoi@tcd.ie

Abstract

Cold Spray (CS) is a rapidly developing metal deposition technology, which allows for the formation of coating layers in a melt-free manner and is starting to replace existing technologies at industrial level. New developments in the field of CS as well as optimization of spraying strategy permit to elaborate freeform 3D objects with reasonable precision. Residual stress is among the most important factors affecting coating integrity in fact they can lead to peeling and/or delamination of coatings. In this study two different types of simulation were performed: at the microscale, using ANSYS-AUTODYN, a high impact simulation in order to study the mechanism of formation of residual stress in the cold-sprayed deposited particle; and at the macroscale a static structural simulation based on Tsui and Clyne's progressive deposition model in order to investigate a possible interaction between different layers and developing a deposition strategy. For the first time, in this work, a parametric study of the single impact particle to study the residual stress was proposed finding that impact velocity; incident angle of impact and density and the yield stress for the materials involved in the deposition have a strong influence in the residual stress formation. Furthermore, at a macroscopic scale, a deposition strategy that minimises residual stress was identified. In fact, it was found that the deposition of successive layers with a perpendicular relative orientation leads to a final product with lower residual stress.

© 2016 The Authors. Published by Elsevier B.V. This is an open access article under the CC BY-NC-ND license (<http://creativecommons.org/licenses/by-nc-nd/4.0/>).

Peer-review under responsibility of the scientific committee of the 5th CIRP Global Web Conference Research and Innovation for Future Production

Keywords: Cold Spray; residual stresses; Deposition; Particle impact; FEA.

1. Introduction

Cold Spray (CS) is a novel metal deposition technology, which allows for the formation of coating layers in a melt-free manner and is starting to replace existing technologies at industrial level. This CS process is an exciting new spray technology that has the potential to overcome limitations of more traditional thermal spray processes for some important commercial applications. It is possible to rapidly deposit thin or very thick layers of a wide range of metals, and even some composite materials, without melting or vaporization, at or near room temperature, in an ambient air environment [1].

In CS inert gases (such as Nitrogen or Helium) are fed at high pressure in the inlet of a supersonic nozzle. The gas expands in the nozzle, and can reach at the exit velocities well above 3600Km/h. Such high speed jet is used to accelerate small metal particles, which are made to strike upon a substrate material. If a threshold energy level is reached at impact, the particles will bond to the substrates and form a coating. New developments in the field of CS as well as optimization of spraying strategy permit to elaborate freeform 3D objects with reasonable precision. The great advantage of CS is its ability to fabricate multi-material, intermetallic, and functionally graded components. However, further work is needed to develop the process and to address challenging

technological issue such as stable powder feeding and optimization of spraying strategy [2].

Residual stress is among the most important factors affecting coating integrity; it can lead to peeling and/or delamination of coatings. Thus, understanding of the bonding mechanism together with the stress formation is critical for improving the overall integrity or performance of the deposition. Up to now, there is a limited amount of data detailing the residual stresses in cold-sprayed materials whether inside a single-deformed particle or the whole coating, though there have been several investigations on residual stress of thermal sprayed coatings. For CS, Tsui and Clyne developed a model [3] capable of predicting the residual stresses profile through the thickness of the deposition. Numerical simulations of a single particle splat [4,5], multi-particle impact [6,7] and single pass [4] are present in literature.

Deposition strategies that minimise residual stresses have already been developed and present in literature for thermal spray, giving more emphasis to the effect of the temperature distribution on the substrate, that is irrelevant in CS application; or simply optimizing the spray angle, the relative speed and distance between torch and component and maintaining them constants during the manufacturing process [8-10]. From the literature review emerged that although CS is rapidly imposing itself as a promising technique for additive manufacturing application, few researches tried to develop a deposition strategy that has as objective the minimisation of residual stress.

Moreover, only the influence of variation of impact velocity, initial temperature and the utilisation of materials such as aluminium and copper has been analysed on the mechanism of formation of residual stress in CS. For this reason, in this study, the implementation of different numerical approaches for the single particle impact was conducted in ANSYS-AUTODYN and then, the analysis of the effects of oblique impact, variation of friction coefficient and the utilisation of titanium together with aluminium and copper, was performed for a better understanding of the mechanism of formation of residual stress.

2. Model Description

2.1. Single Particle Impact

The residual stress derived by the single particle impact was simulated in this study, using the commercial software ANSYS-AUTODYN. The simulations of the parametric study were performed using the Lagrangian model.

Table 1 presents the outline of the parametric study, focusing on the four parameters: materials combination, orientation of impact, impact velocity and frictional coefficient. The values of size, velocity and friction coefficient are typical values present in the literature for this type of analysis.

In order to model the complex response of materials to dynamic loading in our particular study, two components are needed: an equation of state that describes the hydrodynamic response of a material and material strength laws that describe the nonlinear elastic-plastic behaviour.

SHOCK EQUATION OF STATE (EOS) LINEAR:

This model uses a Mie-Gruneisen form of the equation of state based on the shock Hugoniot. The pressure p is determined as a function of density ρ and the specific energy E by:

$$p = p_H + \Gamma \rho (E - E_H) \quad (1)$$

Where it is assumed that:

$$\Gamma = \Gamma_0 \frac{\rho_0}{\rho} \quad (2)$$

$$p_H = \frac{\rho_0 c_1^2 \mu (1 + \mu)}{[1 - (s_1 - 1)\mu]^2} \quad (3)$$

$$E_H = \frac{1}{1} \frac{p_H}{\rho_0} \left(\frac{\mu}{1 + \mu} \right) \quad (4)$$

Where p_H and p_H are the Hugoniot pressure and specific energy; Γ the Gruneisen ratio; Γ_0 a material constant; ρ_0 the reference density; $\mu = -1 + \rho/\rho_0$ the compression and c_1 and s_1 define the linear relationship between the linear shock velocity U_s and the particle velocity U_p as follow:

$$U_s = c_1 + s_1 U_p \quad (5)$$

JOHNSON-COOK STRENGTH:

This is the most suitable model to represent the strength behaviour of materials, typically metals, subjected to large strains, high strain rates and high temperatures, as it happens in our simulation. With this model, the yield stress varies depending on strain, strain rate and temperature.

The model defines the yield stress Y as:

$$Y = [A + B \varepsilon^n][1 + C \ln \dot{\varepsilon}^*][1 - T^{*m}] \quad (6)$$

Where ε is the equivalent plastic strain; $\varepsilon^{*-} = \dot{\varepsilon}/\dot{\varepsilon}_0$ is the dimensionless plastic strain rate for $\dot{\varepsilon}_0 = 1.0s^{-1}$; $T^* = (T - T_0)/(T_m - T_0)$ is the corresponding temperature; n is the work hardening exponent; A , B , C , and m are material constants; T is the temperature in Kelvin; T_m is the melting temperature of the material; and T_0 is a reference temperature.

We assumed a perfectly spherical shape for the particle of Al, Cu and Ti as indicated by scanning electron microscope (SEM) observations present in the literature [12]. In the simulations, the height and radius of the substrate has been chosen to be ten times larger than the particle radius in order to reduce the number of elements of the mesh and therefore the calculation time. Moreover, it has been made sure that the

Table 1: Calculation Plan for the effect of the parameters.

Parameter	Size(μm)	Material	Velocity (m/s)	Orientation ($^\circ$)	Friction	Reference
Orientation	25	Cu/Al	500	0-15-30-45-60	0.3	-
Material	20	Al/Al-Cu/Cu-Ti/Ti-Al/Cu-Cu/Al-Ti/Cu-Cu/Ti-Ti/Al-Al/Ti	500	0	0.3	[11]

extent of the substrate was large enough to eliminate the constraints of the boundary conditions. In fact, the reflective waves from the substrate bottom and far edges would reach the impact zone only after the rebound of the particle.

The radius of the particle has been fixed at 20-25 μm ; the height and radius of the substrate are equals to 125 μm .

A boundary condition that fixed the general velocity of the lateral edge of the substrate at zero value has been applied. An initial velocity has been applied to the particle.

Figure 1 shows the mesh employed for the Lagrangian and ALE models. In order to obtain accurate simulation results with the minimum time needed, an optimized mesh has been employed: elements of size 0.5 μm have been applied to the particle and a redefined zone of 25 μm ×25 μm of the substrate near the impact.

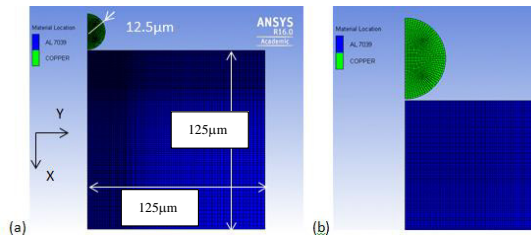


Figure 1: Global Geometry and Mesh representation (a) and detail (b) of the 2D axisymmetric Lagrangian model.

2.2. Multi-layer Deposition

A static structural simulation using ANSYS was performed in order to study the interaction between layer deposited and the influence of different deposition strategies in the final state of residual stress. The basis of our analysis of residual stress accumulation is according to Tsui and Clyne's progressive coating deposition model [3, 13, 14]. In fact, we use this model in order to induce residual stress in each layer. This analytical model is based on force and moment balance and it is capable of predicting the residual stresses profile through the thickness of the deposition, taking into account two main sources of residual stresses: quenching and differential thermal contraction. Since, as

already discussed in the literature review, the model was developed for thermal spray applications and its applicability to CS has been proven in various analyses [4, 7, 15] and, furthermore, it was found that the contribution of the thermal residual stress can be neglected [16]; the model was used in this study to find the loads to apply to each deposited layer. These loads were applied to the geometry and the influence of a different relative orientation of successive layers has been analysed.

A tensile force with this magnitude acts on the deposit while a compressive force of the same magnitude acts on the substrate. This result is extended to the following layers, giving the force for each deposited layer:

$$F_n = \sigma_d b w \left(\frac{H E_s + (n-1) w E_d}{H E_s + n w E_d} \right) \quad (7)$$

While the compressive force is shared between the precedent layers and the substrate with the individual forces, respectively $F_{n,w}$ and $F_{n,s}$, acting on their own neutral axis. These forces are equal to:

$$F_{n,s} = \frac{E_s H F_n}{E_s H + E_d (n-1) w} \quad (8)$$

$$F_{n,w} = \frac{E_d (n-1) w F_n}{E_s H + E_d (n-1) w} \quad (9)$$

Finally, converting the forces into pressures, by dividing them by the area in which they act, simplify the identification of a unique condition for each layer.

Interestingly, the forces and therefore the residual stress described by Tsui and Clyne's model depend only on the final thickness of the deposition and not on the number of individual layers. However, since the residual stress is evaluated at the midpoint of the layer, a larger number of subdivisions results in a higher number of locations in which the residual stress is evaluated and therefore a more accurate distribution of stress. For this reason each layer was divided into 5 sub-divisions.

Figure 2 shows the simulation schematic of two consecutive layers, at a different angle of deposition. By following the above, as each layer has 5 subdivisions, the total of such brings up to 10.

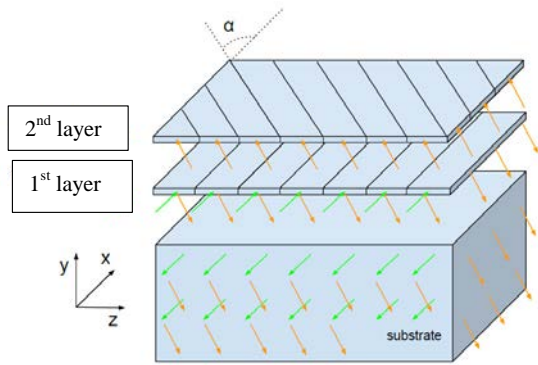


Figure 2: Schematic depiction of geometry and loadings of the static structural analysis.

In this study, we used the two physical parameters of the model σ_d and $\Delta\epsilon$ that Lunzin et al [15] obtained by fitting the model to experimentally measured stress profiles.

3. Results and Discussion

3.1. Residual stress in a Single Particle Impact

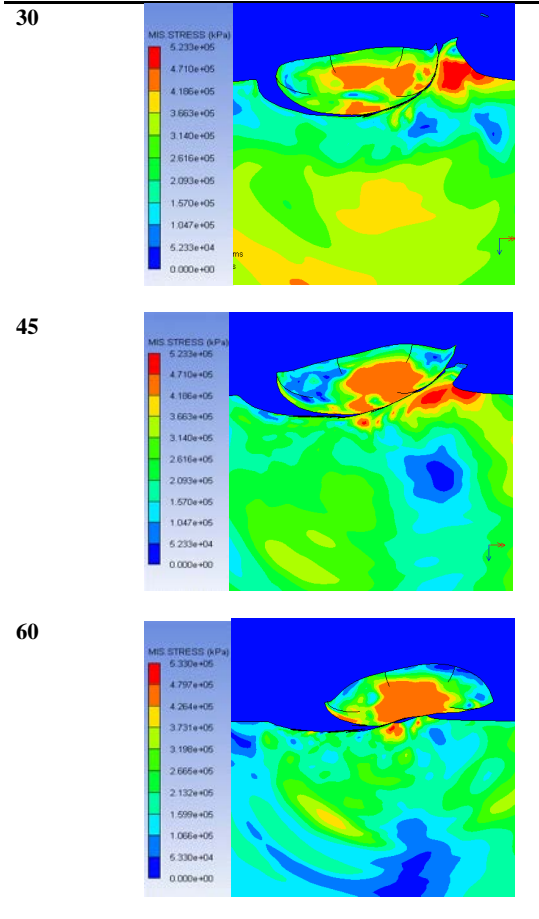
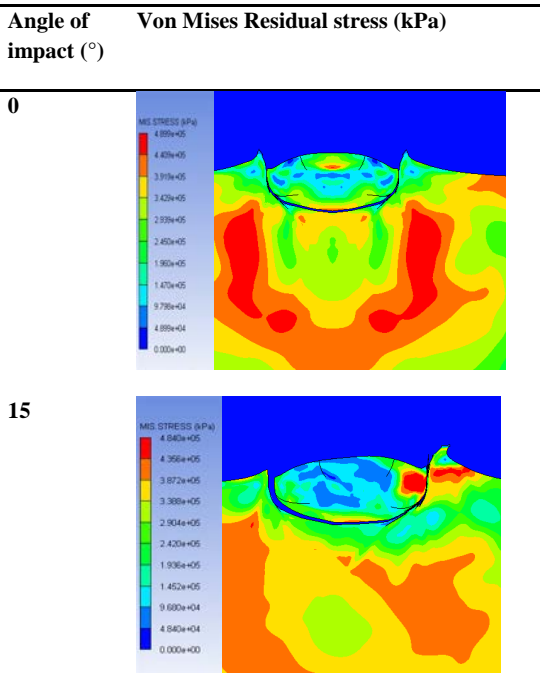


Figure 3: The simulation results for Von Mises stress in a single splat of Cu onto Al at 25°C, with friction coefficient of 0.3, particle velocity of 500 m/s and angle of impact: (a) 0°, (b) 15°, (c) 30°, (d) 45°, and (e) 60°.

From Figure 3 where the results simulation for different angles of impact are shown, it is possible to observe that a smaller incident angle resulted in a shallower dent and a higher pile-up residing ahead of the shot.

It is found that a larger incident angle results in a larger compressive zone and a larger residual stress. These tendencies were similar to those obtained by Yang et al. in [17].

On the other hand, a smaller plastic strain and a larger plastic zone were observed for a larger incident angle. This relates directly to the effective velocity components.

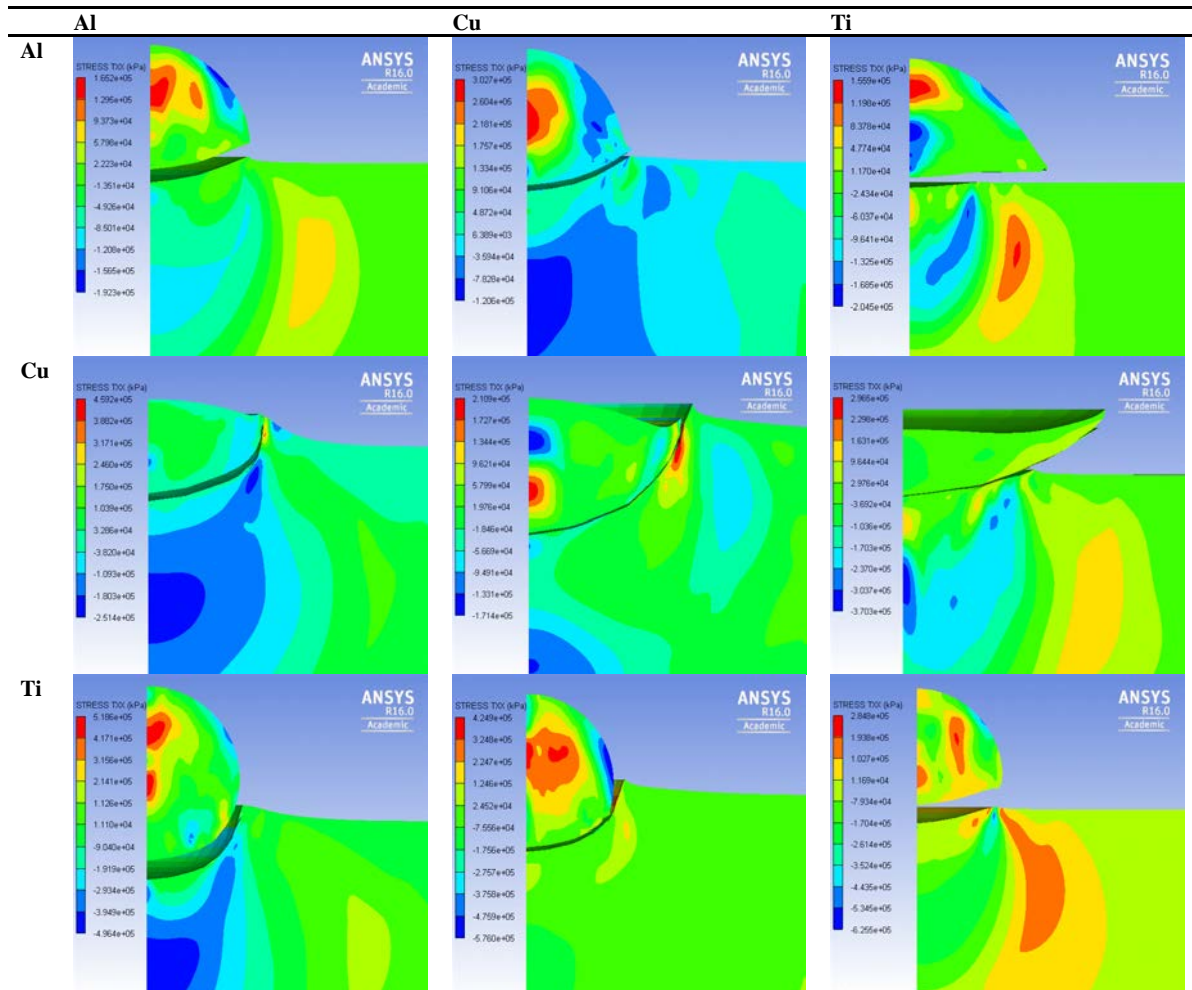


Figure 4: Matrix with in rows particle material and in column substrate material of the simulation results of normal residual stress σ_{xx} of final state at 25°C and with friction coefficient of 0.3 and particle velocity of 500 m/s, in a single splat.

Different combinations of the substrate and coating materials enabled an analysis of the different factors affecting the residual stress state.

From the results in Figure 4, a gap between the particle and the substrate can be noticed, and that represents the rebound. The gap between the particle and the substrate is due to the lack of an adhesion model in the simulation. In reality, if the velocity of impact is higher than the critical velocity described above, metallurgical bonding occurs between the particle and the substrate. The simulation is not able to take into account this mechanism; however the effect on residual stresses computation within the bulk is assumed negligible.

It is interesting to compare the simulation results reported in Figure 4 (deposited×substrate material) in terms

of final state normal residual stress, to the properties of materials reported in Table 2.

Table 2: Properties of Al, Cu and Ti.

	Al	Cu	Ti
Density (kg/m³)	2.77	8.9	4.51
Yield Stress (Mpa)	337	120	850
Brinell Hardness	184	520	1028

It is possible to observe that the density of the material plays an important role in the final configuration of residual stress. In fact, under the same impact conditions the particle

undergoing higher deformation is the Cu particle owing to its higher density and thus more kinetic energy upon impact. However, density is not the only material property affecting the particle deformation. In fact, we can notice that even if titanium has a higher density than aluminium, thus a higher kinetic energy, it deforms less. In effect, the deformation behaviour of both particle and substrate is also dependent on the yield stress. The depth of penetration, deformation and stress can be interpreted by combining the effects of these two material properties.

In addition, these results are in accordance with the reported results [16] that also argued the strong influence of the yield stress in the formation of residual stresses.

The deformation behaviour of Al particles is different to Cu particles under the same impact conditions owing to its lower density and thus less kinetic energy upon impact. Aluminium particles need a higher velocity to reach the same compression ratio as that of Cu particles. With increasing the impact velocity the compression ratio of Al particles increases linearly [18]

3.2. Residual stress in a Multi-layer Deposition



Figure 5: Through-thickness equivalent residual stress profiles for Al layers deposited on Al substrate.

Figure 5 to 8 show simulations carried out with different material combinations, and at 0°, 30°, 60° and 90° relative angles. These angles were chosen to reflect a good distribution across the possible range. Comparing the results for same (Al/Al, Cu/Cu) and different materials (Al/Cu, Cu/Al) cases, we can observe that for the same material cases at the interface the stress has the same value and the profile is continuous while for the different material cases is possible to observe a discontinuity of stress at the interface. This is due to the different materials properties that, therefore, translate into different answers to the loadings. The equivalent stress is higher in the copper whether it is present on the substrate or in the deposition because of its higher Young's Modulus.

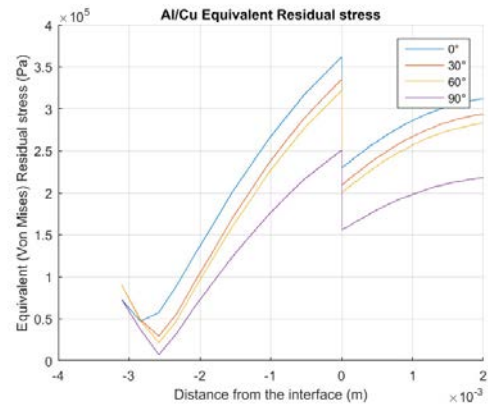


Figure 6: Through-thickness equivalent residual stress profiles for Al layers deposited on Cu substrate.

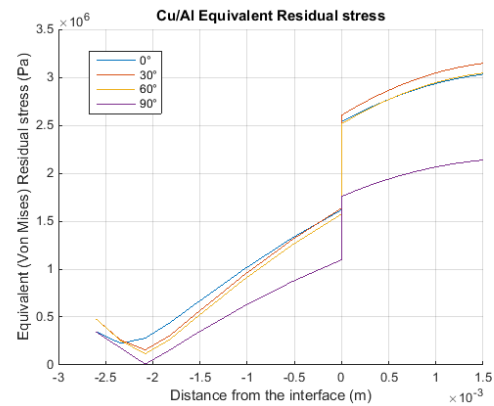


Figure 7: Through-thickness equivalent residual stress profiles for Cu layers deposited on Al substrate.

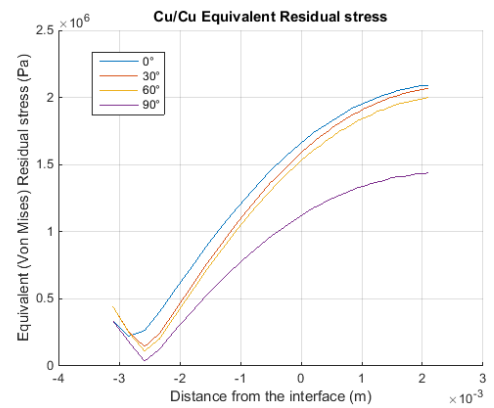


Figure 8: Through-thickness equivalent residual stress profiles for Cu layers deposited on Cu substrate.

More precisely, it is possible to observe that:

- For the Al/Al case (Figure 5) we have the highest equivalent stress in the deposition, the final stress decreases non-linearly while increasing the relative orientation and it is lower for 90°. More precisely, at 90° the maximum equivalent stress is 32% lower than a relative orientation angle of 0°.

- For the Al/Cu case (Figure 6) the final stress decreases non-linearly while increasing the relative orientation and it is lower for 90°. More precisely, at 90° the maximum equivalent stress is 30.5% lower than a relative orientation angle of 0°.

- For the Cu/Al case (Figure 7), while a trend cannot be identified between the different relative orientation angles and the residual stress profiles, the final stress is lower for 90°. More precisely, at 90° the maximum equivalent stress is 32% lower than a relative orientation angle of 0°.

- For the Cu/Cu case (Figure 8), the final equivalent stress decreases non-linearly while increasing the relative orientation. However, they are both lower for 90°. More precisely, at 90° the maximum equivalent stress is 31% lower than a relative orientation angle of 0°.

It is interesting restating that for the four different setups we obtain the same percentage of decrease in residual stress of around 30%.

From a global analysis of stress for an orientation of 0° we can observe that in the case of the Cu coatings a higher residual stress accumulation than in the Al coatings suggest the amount of plasticity on impact is more significant in Cu coatings. The residual stress accumulation in the CS coatings examined here is primarily a result of plastic deformation resulting from particle impact, and thermal effects are relatively minor.

It is found that, while a uniform behaviour for relative angle of orientation between 0° and 90° cannot be identified, the through-thickness residual stress are lower when successive layers are deposited with perpendicular orientation to each other, i.e. with a relative angle of orientation of 90°. In fact, we assist at a compensation of loads in different directions that result in a product with less residual stress, instead of an increase in stress due to the addition of the deposition effect of layers in the same direction.

The deposition strategy that considers a perpendicular deposition of successive layers was proven to result in a compensation of residual stress, conducting to a final product with lesser levels.

4. Conclusion

In order to find a deposition strategy that allows to minimise residual stress in material deposited by CS, allowing a better performance of this technology for addition manufacturing applications, at the microscale the influence of different parameters was analysed through a

single particle impact realised with the commercial software ANSYS-AUTODYN and at the macroscale residual stress were induced in deposited layers thanks to Tsui and Clyne's progressive deposition model and the influence of different orientation of successive layers was analysed.

For the first time, in this work, a parametric study of the single impact particle to study the residual stress was proposed.

From the single impact simulation emerged that:

- A larger incident angle results in a larger compressive zone and a larger residual stress;
- The density and the yield stress of the materials involved in the deposition have a strong influence in the residual stress formation of the CS material.

Although it was shown that materials are among the most important factor which affect the deposition process, it is not possible to categorize the utilisation of a determinate material because the choice of material strongly depends on the component application, its lifecycle, machining costs.

Instead, the macroscopic simulation resulted in the identification of a deposition strategy that is independent of the materials employed for the deposition and substrate. This strategy consists in deposition of successive layers with a perpendicular orientation to each other, i.e. with a relative orientation of 90° between successive levels of layers; and it is able to achieve maximum equivalent stress up to 32% lower than a relative orientation angle of 0° for combination of aluminium and copper depositions. Future work will include the experimental confirmation of the findings reported in this article.

References

- [1] K. Sakaki, "Cold spray process - overview and application trends," *Materials Science Forum*, vol. 449-452, pp. 1305-8, / 2004.
- [2] A. Sova, S. Grigoriev, A. Okunkova, and I. Smurov, "Potential of cold gas dynamic spray as additive manufacturing technology," *International Journal of Advanced Manufacturing Technology*, vol. 69, pp. 2269-2278, 2013.
- [3] Y. C. Tsui and T. W. Clyne, "An analytical model for predicting residual stresses in progressively deposited coatings Part 1: Planar geometry," *Thin Solid Films*, vol. 306, pp. 23-33, 8/ 1997.
- [4] W. Li, K. Yang, D. Zhang, and X. Zhou, "Residual Stress Analysis of Cold-Sprayed Copper Coatings by Numerical Simulation," *Journal of Thermal Spray Technology*, pp. 1-12, 2015/09/22 2015.
- [5] D. Nélias, J. Xie, H. Walter-Le Berre, Y. Ichikawa, and K. Ogawa, "Simulation of the Cold Spray Deposition Process for Aluminum and Copper using Lagrangian, ALE and CEL Methods," in *Thermomechanical Industrial Processes: Modeling and Numerical Simulation*, ed. 2014, pp. 321-358.
- [6] R. Ghelichi, S. Bagherifard, D. Macdonald, I. Fernandez-Pariente, B. Jodoin, and M. Guagliano, "Experimental and numerical study of residual stress evolution in cold spray coating," *Applied Surface Science*, vol. 288, pp. 26-33, 2014.
- [7] M. Saleh, V. Luzin, and K. Spencer, "Analysis of the residual stress and bonding mechanism in the cold spray technique using experimental and numerical methods," *Surface and*

- Coatings Technology*, vol. 252, pp. 15-28, 2014.
- [8] R. Gadow, A. Candel, and M. Floristán, "Optimized robot trajectory generation for thermal spraying operations and high quality coatings on free-form surfaces," *Surface and Coatings Technology*, vol. 205, pp. 1074-1079, 11/15/ 2010.
- [9] A. Candel and R. Gadow, "Advanced robot programming and coupled numerical simulation of heat transfer for thermal spraying," in *Proceedings of the International Thermal Spray Conference*, 2009, pp. 487-491.
- [10] R. Gadow and M. Floristán, "Manufacturing engineering in thermal spraying by advanced robot systems and process kinematics," in *Future Development of Thermal Spray Coatings: Types, Designs, Manufacture and Applications*, ed. 2015, pp. 259-280.
- [11] P. C. King, S. H. Zahiri, and M. Jahedi, "Focused ion beam micro-dissection of cold-sprayed particles," *Acta Materialia*, vol. 56, pp. 5617-5626, 11// 2008.
- [12] T. Suhonen, T. Varis, S. Dosta, M. Torrell, and J. M. Guilemany, "Residual stress development in cold sprayed Al, Cu and Ti coatings," *Acta Materialia*, vol. 61, pp. 6329-6337, 2013.
- [13] Y. C. Tsui and T. W. Clyne, "An analytical model for predicting residual stresses in progressively deposited coatings Part 2: Cylindrical geometry," *Thin Solid Films*, vol. 306, pp. 34-51, 8// 1997.
- [14] Y. C. Tsui and T. W. Clyne, "An analytical model for predicting residual stresses in progressively deposited coatings Part 3: Further development and applications," *Thin Solid Films*, vol. 306, pp. 52-61, 8// 1997.
- [15] V. Luzin, K. Spencer, and M. X. Zhang, "Residual stress and thermo-mechanical properties of cold spray metal coatings," *Acta Materialia*, vol. 59, pp. 1259-1270, 2011.
- [16] K. Spencer, V. Luzin, N. Matthews, and M. X. Zhang, "Residual stresses in cold spray Al coatings: The effect of alloying and of process parameters," *Surface and Coatings Technology*, vol. 206, pp. 4249-4255, 5/25/ 2012.
- [17] F. Yang, Z. Chen, and S. A. Meguid, "3D FE modeling of oblique shot peening using a new periodic cell," *International Journal of Mechanics and Materials in Design*, vol. 10, pp. 133-144, 2014.
- [18] W.-Y. Li, H. Liao, C.-J. Li, H.-S. Bang, and C. Coddet, "Numerical simulation of deformation behavior of Al particles impacting on Al substrate and effect of surface oxide films on interfacial bonding in cold spraying," *Applied Surface Science*, vol. 253, pp. 5084-5091, 3/30/ 2007.